Inorg. Chem. **2005**, *44*, 8581–8586

Efficient Photoreduction Process of $[Ru_3(\mu_3\text{-}O)(\mu\text{-}CH_3CO_2)_6L_3]^+$ by Electron-Mediation via the Viologen Dication by Excitation of a Zinc Porphyrin

Midoriko Otake,[†] Mitsunari Itou,[†] Yasuyuki Araki,[†] Osamu Ito,*[,†] and Hiroaki Kido[‡]

Institute of Multidisciplinary Research for Advanced Materials, Tohoku University, Katahira, Aoba-ku, Sendai, 980-8577, Japan, and Department of Materials Chemistry, College of Engineering, Nihon University, Tamura-machi, Kouriyama, 963-8642, Japan

Received June 14, 2005

Photoinduced electron-transfer and electron-mediation processes from the excited triplet state of zinc tetraphenylporphyrin (^{3}ZnTPP*) to the hexyl viologen dication (HV^{2+}) in the presence of oxo-acetato-bridged triruthenium clusters, $[Ru_3(\mu_3\text{-}O)(\mu\text{-}CH_3CO_2)_6L_3]^+$, have been revealed by the transient absorption spectra in the visible and near-IR regions. By the nanosecond laser-flash photolysis of ZnTPP in the presence of HV^{2+} and $[Ru_3(\mu_3\text{-}O)(\mu\text{-}CH_3CO_2)_6L_3]^+$, the transient absorption bands of the radical cation of ZnTPP ($ZnTPP^{\bullet+}$) and the reduced viologen ($HV^{\bullet+}$) were initially observed with the concomitant decay of ^{3}ZnTPP*, after which an extra electron of $HV^{\bullet+}$ mediates to $[Ru_3(\mu_3\text{-}O)(\mu\text{-}CH_3CO_2)_6L_3]^+$, efficiently generating $[Ru_3(\mu_3\text{-}O)(\mu\text{-}CH_3CO_2)_6L_3]^0$ with high potential. Although back-electron transfer took place between $ZnTPP^{\bullet+}$ and $[Ru_3(\mu_3\text{-}O)(\mu\text{-}CH_3CO_2)_6L_3]^0$ in the diffusion-controlled limit, $[Ru_3(\mu_3\text{-}O)(\mu\text{-}CH_3CO_2)_6L_3]^0$ accumulates at a steady concentration upon further addition of 1-benzyl-1,4-dihydronicotinamide (BNAH) as a sacrificial donor to re-produce ZnTPP from $ZnTPP^{\bullet+}$. Therefore, we established a novel system to accumulate $[Ru_3(\mu_3\text{-}O)(\mu\text{-}CH_3CO_2)_6L_3]^0$ as an electron pool by the excitation of ZnTPP as photosensitizing electron donor in the presence of HV^{2+} and BNAH as an electron-mediating reagent and sacrificial donor, respectively. With the increase in the electron-withdrawing abilities of the ligands, the final yields of $[Ru_3(\mu_3\text{-}O)(\mu\text{-}CH_3CO_2)_6L_3]^0$ increased.

Introduction

Multinuclear metal complexes have recently attracted considerable interest for supramolecular chemistry using the characteristics of the coordination bonds; the multinuclear metal complexes are widely applicable to nanometer-scale devices and active catalyst.[1] Thus, many kinds of the multinuclear complexes containing two or more metals and various types of ligand have been synthesized, and their electrochemical, optical, and photophysical properties have been widely studied.[2] In particular, photoinduced electron-transfer systems aiming at artificial photosynthesis,[3] photocatalysts,[4] and hydrogen gas evolution from water[5] have been studied to solve environmental problems. For conversion of

* To whom correspondence should be addressed. E-mail: ito@tagen.tohoku.ac.jp. Phone, Fax: +81-22-217-5608.

[†] Tohoku University.

[‡] Nihon University.

(1) (a) Takagi, S.; Inoue, H. In *Molecular and Supramolecular Potochemistry*; Ramamurthy, V., Schanze, K. S., Eds.; Marcel Dekker: New York, 1999; Vol. 4, Chapter 6. (b) Astruc, D. *Electron Transfer and Radical Processes in Transition-Metal Chemistry*; VCH Publishers: New York, 1995. (c) Feringa, B. L. *Molecular Switches*; Wiley-VCH: Weinheim, Germany, 2001. (d) O'Regan, B.; Grätzel, M. *Nature* **1991**, *353*, 737−740.

(2) (a) May, V.; Kühn, O. *Charge and Energy Transfer Dynamics in Molecular Systems*; Wiley-VCH: Heppenheim, Germany, 2004. (b) Guldi, D. M.; Maggini, M.; Menna, E.; Scorrano, G.; Ceroni, P.; Marcaccio, M.; Paolucci, F.; Roffia, S. *Chem.—Eur. J.* **2001**, *7*, 1597−1605. (c) Borgström, M.; Johansson, O.; Lomoth, R.; Baudin, H. B.; Wallin, S.; Sun, L.; Åkermark, B.; Hammarström, L. *Inorg. Chem.* **2003**, *42*, 5173−5184. (d) Fukuzumi, S.; Okamoto, K.; Gros, C. P.; Guilard, R. *J. Am. Chem. Soc.* **2004**, *126*, 10441−10449. (e) Gholamkhass, B.; Mametsuka, H.; Koike, K.; Tanabe, T.; Furue, M.; Ishitani, O. *Inorg. Chem.* **2005**, *44*, 2326−2336.

(3) (a) Imahori, H.; Tamaki, K.; Guldi, D. M.; Luo, C.; Fujitsuka, M.; Ito, O.; Sakata, Y.; Fukuzumi, S. *J. Am. Chem. Soc.* **2001**, *123*, 2607−2617. (b) Imahori, H.; Guldi, D. M.; Tamaki, K.; Yoshida, Y.; Luo, C.; Sakata, Y.; Fukuzumi, S. *J. Am. Chem. Soc.* **2001**, *123*, 6617−6628. (c) Imahori, H.; Tamaki, K.; Araki, Y.; Sekiguchi, Y.; Ito, O.; Sakata, Y.; Fukuzumi, S. *J. Am. Chem. Soc.* **2002**, *124*, 5165−5174. (d) Imahori, H. *Org. Biomol. Chem.* **2004**, *2*, 1425−1433. (e) D'Souza, F.; Deviprasad, G. R.; El-Khouly, M. E.; Fujitsuka, M.; Ito, O. *J. Am. Chem.* Soc. **2001**, *123*, 5277−5284. (f) D'Souza, F.; Smith, P. M.; Zandller, M. E.; McCarty, A. L.; Itou, M.; Araki, Y.; Ito, O. *J. Am. Chem. Soc.* **2004**, *126*, 7898−7907.

10.1021/ic050960s CCC: $30.25
Published on Web 10/04/2005

Chart 1

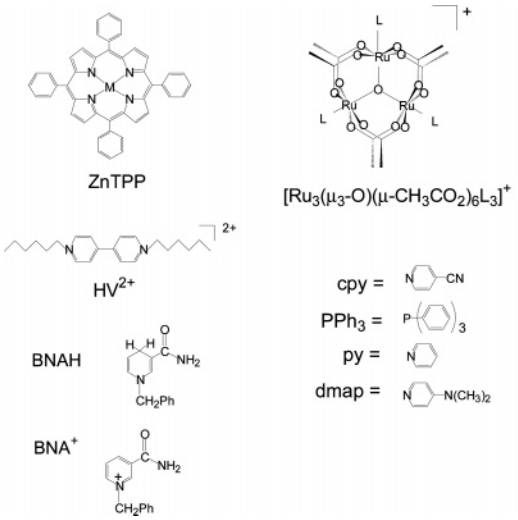

the light energy to chemical energy, it is important to utilize the charge-separated states generated after the photoexcitation of the antenna molecules. Thus, it is quite important to control these processes for the development of the efficient molecular devices. To control these photochemical and photophysical processes, multinuclear metal complexes such as $[Ru_3(\mu_3\text{-}O)(\mu\text{-}CH_3CO_2)_6L_3]^{n+}$ (Chart 1) are interesting molecules because most of the characteristic properties in the absorption spectra and electrochemical studies of this type of cluster complex are quite sensitive to the terminal ligand (L) and total charge.[6,7]

In the previous study,[8] we reported that the photoinduced intermolecular electron transfer from the triplet excited states of zinc tetraphenylporphyrin (^{3}ZnTPP*) or zinc tetra-*tert*-butylphthalocyanine (^{3}ZnTBPc*) could be used as photosensitizing electron-donors to $[Ru_3(\mu_3\text{-}O)(\mu\text{-}CH_3CO_2)_6L_3]^+$, generating transiently $[Ru_3(\mu_3\text{-}O)(\mu\text{-}CH_3CO_2)_6L_3]^0$. Furthermore, we demonstrated that the control of photoinduced electron-transfer rate constants (k_{ET}) and quantum-yields (Φ_{ET}) could be achieved by exchanging the terminal ligands (L). In the case of ^{3}ZnTPP*, however, the quantum yields of the electron-transfer process are not high because there may be an excited energy deactivation process of ^{3}ZnTPP* by $[Ru_3(\mu_3\text{-}O)(\mu\text{-}CH_3CO_2)_6L_3]^+$, competitive with the aimed electron-transfer process.

Herein, we report an attempt to generate $[Ru_3(\mu_3\text{-}O)(\mu\text{-}CH_3CO_2)_6L_3]^0$ from $[Ru_3(\mu_3\text{-}O)(\mu\text{-}CH_3CO_2)_6L_3]^+$ by an indirect method using an electron-mediating strategy, while avoiding the deactivation process of ^{3}ZnTPP* by $[Ru_3(\mu_3\text{-}O)(\mu\text{-}CH_3CO_2)_6L_3]^+$. For this aim, we selected the hexyl viologen dication (HV^{2+}) as an initial electron-acceptor versus ^{3}ZnTPP* and as an electron-mediator to $[Ru_3(\mu_3\text{-}O)(\mu\text{-}CH_3CO_2)_6L_3]^+$. For accumulation of $[Ru_3(\mu_3\text{-}O)(\mu\text{-}CH_3CO_2)_6L_3]^0$ as an electron pool, we revealed the usefulness of 1-benzyl-1,4-dihydronicotinamide (BNAH) as a sacrificial donor, which is converted to stable 1-benzyl-nicotinamidiniumion (BNA^+) after donating an electron to the radical cation of ZnTPP ($ZnTPP^{\bullet+}$).

Experimental Section

Materials. Commercially available acetonitrile (AN) and benzonitrile (BN), used as solvents, and 1-benzyl-1,4-dihydronicotinamide (BNAH), used as a sacrificial donor, were the best grade reagents. Tetra-*n*-butylammonium hexafluorophosphate ($(n\text{-}C_4H_9)_4N^+PF_6^-$), used as a supporting electrolyte in the electrochemical measurements, was recrystallized from ethyl acetate/benzene (1:1 *v*/*v*).[9] Zinc tetraphenylporphyrin (ZnTPP),[10] hexyl viologen perchlorate ($HV^{2+}ClO_4^{2-}$),[11] and $[Ru_3(\mu_3\text{-}O)(\mu\text{-}CH_3CO_2)_6L_3]PF_6$[6d,12] were prepared by the reported methods. As ligands, commercially available 4-cyanopyridine (cpy), triphenylphosphine (PPh_3), pyridine (py), and 4-(dimethylamino)pyridine (dmap) were employed.

Apparatus. Steady-state absorption spectra in the visible and near-IR regions were measured with a Jasco V570 DS spectrophotometer. Nanosecond transient absorption measurements were carried out using a SHG (532 nm) of the Nd:YAG laser (Spectra-Physics, Quanta-Ray GCR-130, fwhm 6 ns) as an excitation source. For measurements in the near-IR region (600−1200 nm), a monitoring light from a pulsed Xe lamp was detected with a Ge-avalanche photodiode (Hamamatsu Photonics, B2834). For transient spectra in the visible region (400−600 nm), a Si−PIN photodiode (Hamamatsu Photonics, S1722−02) was used a detector. Photoinduced events in microsecond time regions were measured using a continuous Xe lamp (150W) and an InGaAs−PIN photodiode (Hamamatsu Photonics, G5125−10) as a probe light and detector, respectively. All the sample solutions in a quartz cell (1 × 1 cm) were deaerated by bubbling Ar gas through the solutions for 15 min.

(4) (a) Hawecker, J.; Lehn, J.-M.; Ziessel, R. *Chem. Commun.* **1983**, 536−537. (b) Hori, H.; Johnson, F. P. A.; Koike, K.; Ishitani, O.; Ibusuki, T. *J. Photochem. Photobiol. A* **1996**, *96*, 171−174. (c) Argazzi, R.; Bignozzi, C. A.; Heimer, T. A.; Meyer, G. J. *Inorg. Chem.* **1997**, *36*, 2−3. (d) Argazzi, R.; Bignozzi, C. A.; Bortolini, O.; Traldi, P. *Inorg. Chem.* **1993**, *32*, 1222−1225. (e) Schoonover, J. R.; Gordon, K. C.; Argazzi, R.; Woodruff, W. H.; Peterson, K. A.; Bignozzi, C. A.; Dyer, R. B.; Meyer, T. J. *J. Am. Chem. Soc.* **1993**, *115*, 10996−10997.

(5) (a) Keller, P.; Moradpour, A. *J. Am. Chem. Soc.* **1980**, *102*, 7193−7196. (b) Keller, P.; Moradpour, A.; Amouyel, E.; Kagan, H. *J. Mol. Catal.* **1980**, *7*, 539−542. (c) Krasna, A. I. *J. Photochem. Photobiol. A* **1980**, *31*, 75−82. (d) Calvert, J. M.; Manuccia, T. J.; Nowak, R. J. *J. Electrochem. Soc.* **1986**, *133*, 951−953. (e) McMahon, R. J.; Force, R. K.; Patterson, H. H.; Wrighton, M. S. *J. Am. Chem. Soc.* **1988**, *110*, 2670−2672. (f) Okura, I., Ed. *Photosensitization of Porphryins and Phthalocyanines.* Gordon and Breach Science Publishers: Amsterdam, 2001.

(6) (a) Walsh, J. L.; Baumann, J. A.; Meyer, T. J. *Inorg. Chim. Acta* **1980**, *19*, 2145−2151. (b) Toma, H. E.; Cunha, C. J.; Cipriano, C. *Inorg. Chim. Acta* **1988**, *154*, 63−66. (c) Ota, K.; Sasaki, H.; Matsui, T.; Hamaguchi, T.; Yamaguchi, T.; Ito, T.; Kido, H.; Kubiak C. P. *Inorg. Chem.* **1999**, *38*, 4070−4078. (d) Toma, H. E.; Araki, K.; Alexiou, A. D. P.; Nikolaou, S.; Dovidauskas, S. *Coord. Chem. Rev.* **2001**, *219*−*221*, 187−234.

(7) (a) Davis, S.; Drago, R. S. *Inorg. Chem.* **1988**, *27*, 4759−4760. (b) Abe, M.; Sasaki, Y.; Yamaguchi, T.; Ito, T. *Bull. Chem. Soc. Jpn.* **1992**, *65*, 1585−1590. (c) Cotton, F. A.; Norman, J. G., Jr. *Inorg. Chim. Acta* **1972**, *6*, 411−419.

(8) Itou, M.; Otake, M.; Araki, Y.; Ito, O.; Kido, H. *Inorg. Chem.* **2005**, *44*, 1580−1587.

(9) Abe, M.; Sasaki, Y.; Yamada, Y.; Tsukahara, K.; Yano, S.; Yamaguchi, T.; Tominaga, M.; Taniguchi, I.; Ito, T. *Inorg. Chem.* **1996**, *35*, 6724−6734.

(10) (a) Adler, A. D.; Longo, F. R.; Finarelli, J. D.; Goldmacher, J.; Assour, J.; Korsakoff, L. *J. Org. Chem.* **1967**, *32*, 476. (b) Fleischer, E. B.; Shachter, A. M. *Inorg. Chem.* **1991**, *30*: 3763−3769.

(11) (a) Monk, P. M. S. *The Viologens*; John Wiley & Sons: Chichester, U.K., 1998. (b) Fukuzumi, S.; Imahori, H.; Yamada, H.; El-Khouly, M. E.; Fujitsuka, M.; Ito, O.; Guldi, D. M. *J. Am. Chem. Soc.* **2001**, *123*, 2571−2575.

(12) (a) Baumann, J. A.; Salmon, D. J.; Wilson, S. T.; Meyer, T. J. *Inorg. Chem.* **1978**, *17*, 3342−3350. (b) Baumann, J. A.; Wilson, S. T.; Salmon, D. J.; Hood, P. L.; Meyer, T. J. *J. Am. Chem. Soc.* **1979**, *101*, 2916−2920.

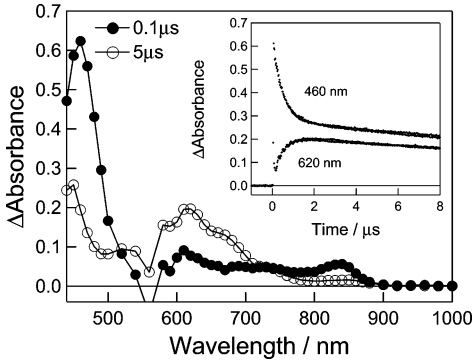

Figure 1. Transient absorption spectra of ZnTPP (0.05 mM) and HV^{2+} (0.5 mM) after 532 nm laser irradiation in Ar-saturated AN. Inset: Absorption−time profiles of ^{3}ZnTPP* at 460 nm and HV^{2+} at 620 nm.

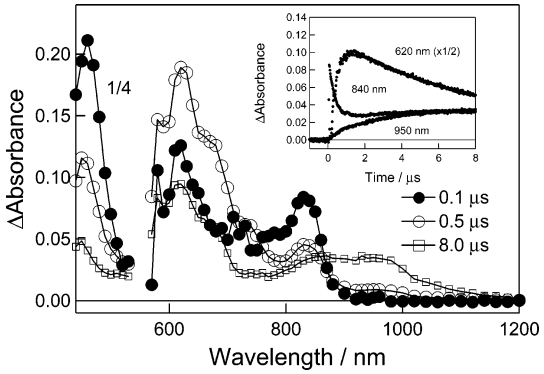

Figure 2. Transient absorption spectra of ZnTPP (0.05 mM), $[Ru_3(\mu_3\text{-}O)(\mu\text{-}CH_3CO_2)_6(cpy)_3]^+$ (0.1 mM), and HV^{2+} (1.0 mM) after 532 nm laser irradiation in Ar-saturated AN. Inset: Absorption−time profiles of ^{3}ZnTPP* decay at 840 nm, $HV^{\bullet+}$ at 620 nm, and $[Ru_3(cpy)_3]^0$ at 950 nm.

Results and Discussion

Photoinduced Electron-Transfer Processes. Transient absorption spectra in the visible and near-IR regions were observed as shown in Figure 1 using the excitation of ZnTPP in the presence of the HV^{2+} in deaerated AN with the laser light at 532 nm, which predominantly excites ZnTPP. Immediately after the laser-light irradiation, the transient absorption bands appeared at 460 and 840 nm, which can be attributed to ^{3}ZnTPP*.[13] With the concomitant decay of ^{3}ZnTPP*, a new absorption band appeared around 620 nm, which was assigned to the absorption band of the radical cation of hexyl viologen ($HV^{\bullet+}$).[14] The absorption band that remained around 440 nm can be attributed to both $ZnTPP^{\bullet+}$ and $HV^{\bullet+}$. The absorption-time profiles (inset of Figure 1) show that the appearance of the absorption band of $HV^{\bullet+}$ at 620 nm corresponds to the initial decay of ^{3}ZnTPP* at 460 nm. Thus, it was clearly indicated that photoinduced electron transfer occurs via ^{3}ZnTPP* as shown in eq 1.[15]

$$^3\text{ZnTPP}^* + \text{HV}^{2+} \xrightarrow{k_{ET},\,\Phi_{ET}} \text{ZnTPP}^{\bullet+} + \text{HV}^{\bullet+} \qquad (1)$$

The absorption intensity of ^{3}ZnTPP* at 460 nm did not decay completely in the longer time region than ca. 1 μs because the absorption tails of $ZnTPP^{\bullet+}$ and $HV^{\bullet+}$ are overlapping with that of ^{3}ZnTPP* at 460 nm; thus, the slow decay rate at 460 nm after ca. 1 μs was the same of the slow decay rate of $HV^{\bullet+}$ at 620 nm, as shown in inset of Figure 1. The initial decay rate of ^{3}ZnTPP* and rate of increase of $HV^{\bullet+}$ gave the first-order rate-constants (k_{first}), which increase with the concentration of added HV^2+, resulting in the bimolecular quenching rate-constant (k_q) of ^{3}ZnTPP* being 1.2×10^{10} M^{-1} s^{-1} from the pseudo-first-order relation. The quantum yield (Φ_{ET}) for electron transfer (eq 1) was evaluated to be 0.95 from the concentration ratio of $[HV^{\bullet+}]/[^3\text{ZnTPP}^*]$ using the observed maximal absorbance and the reported molar extinction coefficients, $\epsilon_{840\,nm} = 8500$ M^{-1} cm^{-1} for ^{3}ZnTPP* [11] and $\epsilon_{620\,nm} = 11\,000$ M^{-1} cm^{-1} for $HV^{\bullet+}$ [16] in AN. Thus, the rate constant for electron transfer (k_{ET}) can finally be calculated to be 1.1×10^{10} M^{-1} s^{-1} from the following relation, $k_{ET} = k_q \times \Phi_{ET}$.

Using the oxidation potential of ZnTPP ($E_{ox} = 0.38$ V vs Fc/Fc^+ in AN), the reduction potential of HV^{2+} ($E_{red} = -0.83$ V vs Fc/Fc^+ in AN), and the lowest-energy level of ^{3}ZnTPP* ($E_{00} = 1.53$ eV), the free- energy change for electron transfer (ΔG_{ET}) was evaluated using the Rehm−Weller equation (eq 2)[17]

$$-\Delta G_{ET} = E_{00} - E_{ox} + E_{red} + E_c \qquad (2)$$

where E_c (eV) refers to the Coulomb energy as calculated by eq 3

$$E_c = (z_D z_A)e^2/23.06 \times d_{cc}\epsilon_s \qquad (3)$$

where z_D and z_A refer to the effective charge of ZnTPP and HV^{2+}, respectively, d_{cc} refers to the collision radius between the two moieties, and ϵ_s refers to the static dielectric constant of AN. The ΔG_{ET} value was determined to be -0.30 eV, supporting the exothermic reaction of eq 1.

For the long time-scale measurements, $HV^{\bullet+}$ begins to decay obeying second-order kinetics, which indicates that the back-electron transfer takes place between $ZnTPP^{\bullet+}$ and $HV^{\bullet+}$ after they are fully solvated by AN (eq 4). The rate constant for the back-electron transfer (k_{BET}) was determined to be 1.0×10^{10} M^{-1} s^{-1} in AN, which is close to the diffusion-controlled limit ($k_{diff} = 1.9 \times 10^{10}$ M^{-1} s^{-1} in AN).[13]

$$\text{ZnTPP}^{\bullet+} + \text{HV}^{\bullet+} \xrightarrow{k_{BET}} \text{ZnTPP} + \text{HV}^{2+} \qquad (4)$$

Electron-Mediating Process. The transient absorption spectra observed by the selective excitation of ZnTPP, upon addition of $[Ru_3(\mu_3\text{-}O)(\mu\text{-}CH_3CO_2)_6L_3]^+$ to the AN solution containing ZnTPP and HV^{2+}, are shown in Figure 2. After the absorption of $HV^{\bullet+}$ at 620 nm reaches a maximal

(13) Murov, S. L.; Carmichael, I.; Hug, G. L. *Handbook of Photochemistry*, 2nd ed; Marcel Dekker: New York, 1993.
(14) (a) Krumholtz, P. *J. Am. Chem. Soc.* **1951**, *73*, 3487−3492. (b) Kosower, E.; Cotter, J. L. *J. Am. Chem. Soc.* **1964**, *86*, 5524−5527. (c) Mohammed, M. *J. Org. Chem.* **1987**, *52*, 2779−2782.
(15) (a) Darwent, J. R.; Douglas, P.; Harriman, A.; Porter, G.; Richoux, M.-C. *Coord. Chem. Rev.* **1982**, *44*, 83−126. (b) Harriman, A. *J. Photochem.* **1985**. *29*, 139−150. (c) Parmon, V. N.; Lymar, S. V.; Tevetkov, L. M.; Zamaraev, K. I. *J. Mol. Catal.* **1983**, *21*, 353−363. (d) Kagner, E.; Joselevich, E.; Willner, I.; Chen, Z.; Gunter, M. J.; Gayness, T. P.; Johnson, M. R. *J. Phys. Chem. B* **1998**, *102*, 1159−1165.
(16) Watanabe, T.; Honda, K. *J. Phys. Chem.* **1982**, *86*, 2617.
(17) Rehm, D.; Weller, A. *Isr. J. Chem.* **1970**, *8*, 259−271.

Table 1. Free-Energy Changes ($-\Delta G_{MED}$), Rate Constants (k_{MED}), Quantum Yields (Φ_{MED}), Total Quantum Yields (Φ_{ET}^{total}) for the Generation of [Ru$_3$(μ_3-O)(μ-CH_3CO_2)$_6$(L)$_3$]^0 via ^{3}ZnTPP*, and Back-Electron Transfer Rate Constants (k_{BET}^{final}) between [Ru$_3$(μ_3-O)(μ-CH_3CO_2)$_6$(L)$_3$]^0 and ZnTPP$^{\bullet+}$ [a]

L	solvent	$-\Delta G_{MED}$[b] (eV) ($HV^{\bullet+} \rightarrow Ru_3L_3^+$)	k_{MED} (M^{-1} s^{-1}) ($HV^{\bullet+} \rightarrow Ru_3L_3^+$)	Φ_{MED}[c] ($HV^{\bullet+} \rightarrow Ru_3L_3^+$)	Φ_{ET}^{total} [d] (^{3}ZnTPP* $\rightarrow Ru_3L_3^+$)	k_{BET}^{final} [e] (M^{-1} s^{-1}) ($Ru_3L_3^0 \rightarrow$ ZnTPP$^{\bullet+}$)
cpy	AN	0.53	8.7×10^8	0.49	0.47	1.7×10^{10}
PPh_3	AN	0.48	7.4×10^8	0.32	0.30	1.7×10^{10}
py	AN	0.37	5.9×10^8	0.29	0.28	1.6×10^{10}
dmap	AN	0.18	5.8×10^8	0.15	0.13	1.7×10^{10}
cpy	BN	0.49	2.1×10^8	0.41	0.39	5.2×10^9
PPh_3	BN	0.40	1.1×10^8	0.34	0.32	4.0×10^9
py	BN	0.29	1.2×10^8	0.31	0.29	5.8×10^9
dmap	BN	0.08	2.2×10^7	<0.1	<0.1	(1.3×10^{10})[f]

[a] Ru$_3$(μ_3-O)(μ-CH_3CO_2)$_6$(L)$_3$ is abbreviated as Ru_3L_3. [b] The ΔG_{MED} values were determined using the Rehm−Weller equation[17] with $E_{red} = -0.83$ eV for HV^{2+} vs Fc/Fc^+ in AN and BN and E_{red} for [Ru$_3$(μ_3-O)(μ-CH_3CO_2)$_6$(L)$_3$]$^+$.[8] [c] $\epsilon = 1.1 \times 10^4$ M^{-1} cm^{-1} at 620 nm for $HV^{\bullet+}$.[16] [d] $\epsilon = 8.5 \times 10^3$ M^{-1} cm^{-1} at 840 nm for ^{3}ZnTPP*.[11b] [e] The ϵ values reported in our previous report[8] were used to calculate k_{BET}^{final}. [f] Estimation was difficult because of the weak signal.

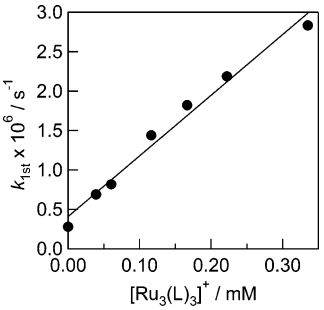

Figure 3. Plot of the pseudo-first-order rate constant for decay of $HV^{\bullet+}$ vs [Ru$_3$(μ_3-O)(μ-CH_3CO_2)$_6$(cpy)$_3$]$^+$ in AN: [Ru$_3$(μ_3-O)(μ-CH_3CO_2)$_6$(cpy)$_3$]$^+$ is abbreviated as [Ru$_3$(L$_3$)]$^+$.

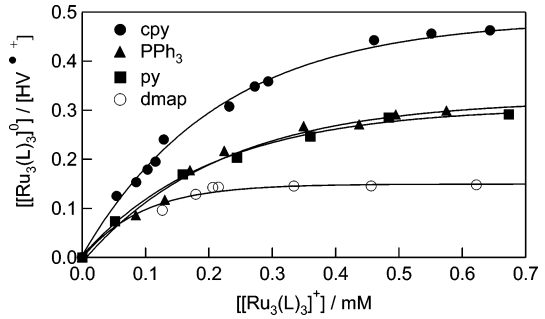

Figure 4. Relations between [Ru$_3$(μ_3-O)(μ-CH_3CO_2)$_6$L$_3$]^0]/[$HV^{\bullet+}$] and the concentration of [Ru$_3$(L)$_3$]$^+$ in AN for various ligands: [Ru$_3$(μ_3-O)(μ-CH_3CO_2)$_6$L$_3$]^0 is abbreviated as [Ru$_3$(L)$_3$]^0.

concentration at ca. 1 μs, which was generated via ^{3}ZnTPP* at 460 and 840 nm as shown in the spectrum at 0.1 μs, a new broad absorption band appeared at 940 nm in the spectrum observed at 8 μs. The 940 nm band can be assigned to [Ru$_3$(μ_3-O)(μ-CH_3CO_2)$_6$L$_3$]^0.[8,18] As shown in the inserted time profile in Figure 2, the first electron-transfer step from ^{3}ZnTPP* to HV^{2+} was completely finished within ca. 1 μs, at which $HV^{\bullet+}$ reached the maximal concentration. With the relatively slow decay of $HV^{\bullet+}$ after ca. 1 μs, the absorption intensity of [Ru$_3$(μ_3-O)(μ-CH_3CO_2)$_6$L$_3$]^0 increased. Therefore, the generation of [Ru$_3$(μ_3-O)(μ-CH_3CO_2)$_6$L$_3$]^0 is attributed to the electron-mediation process from $HV^{\bullet+}$ to [Ru$_3$(μ_3-O)(μ-CH_3CO_2)$_6$L$_3$]$^+$ as shown in eq 5.

$$HV^{\bullet+} + [Ru_3(\mu_3\text{-O})(\mu\text{-}CH_3CO_2)_6L_3]^+ \xrightarrow{k_{MED}} HV^{2+} + [Ru_3(\mu_3\text{-O})(\mu\text{-}CH_3CO_2)_6L_3]^0 \quad (5)$$

The observed first-order rate-constants (k_{first}) for the decay of the absorption of $HV^{\bullet+}$ at 620 nm and the absorption of [Ru$_3$(μ_3-O)(μ-CH_3CO_2)$_6$L$_3$]^0 at 940 nm increase linearly with the concentration of [Ru$_3$(μ_3-O)(μ-CH_3CO_2)$_6$L$_3$]$^+$ as shown in Figure 3, indicating the pseudo-first-order relation for eq 5. From the slope of a linear line in Figure 3, the second-order rate constant, k_{MED}, was determined to be 8.7×10^8 M^{-1} s^{-1}, when L = cpy. For other ligands, the k_{MED} values were similarly determined, as listed in Table 1. The free-energy changes (ΔG_{MED}) were evaluated as the differences between the reduction potentials of HV^{2+} and [Ru$_3$(μ_3-O)(μ-CH_3CO_2)$_6$L$_3$]$^+$, in which the latter values were reported in our previous paper,[8] as listed in Table 1. In AN and BN, the values of ΔG_{MED} are all negative, allowing an exothermic reaction. With an increase in the electron-withdrawing ability of ligands (cpy > PPh_3 > py > dmap), the exothermic energy increases;the k_{MED} values increase in the same order.

To evaluate the quantum yields of the electron-mediating process (Φ_{MED}), the ratio of [Ru$_3$(μ_3-O)(μ-CH_3CO_2)$_6$L$_3$]^0]/[$HV^{\bullet+}$] is plotted against the concentration of [Ru$_3$(μ_3-O)(μ-CH_3CO_2)$_6$L$_3$]$^+$, as shown in Figure 4, in which the saturation of the ratio was observed with increasing concentration of [Ru$_3$(μ_3-O)(μ-CH_3CO_2)$_6$L$_3$]$^+$. The saturated values were attributed to the Φ_{MED} values, which are listed in Table 1. The Φ_{MED} values increase with the electron-withdrawing ability of the ligands. However, the evaluated Φ_{MED} values are all less than 0.5, probably because $HV^{\bullet+}$ was consumed not only by the electron-mediating process (eq 5) but also by the back-electron transfer to ZnTPP$^{\bullet+}$ (eq 4).

The total quantum yields (Φ_{ET}^{total}) for the generation of [Ru$_3$(μ_3-O)(μ-CH_3CO_2)$_6$L$_3$]^0 on the basis of ^{3}ZnTPP* were calculated by $\Phi_{ET} \times \Phi_{MED}$ as listed in Table 1. These Φ_{ET}^{total} values are larger than the corresponding quantum yields (Φ_{ET}^{direct})[8] for direct electron transfer from ^{3}ZnTPP* to [Ru$_3$(μ_3-O)(μ-CH_3CO_2)$_6$L$_3$]$^+$ by a factor of 1.4−1.6. Therefore, the photoinduced electron-mediating method employed in the preset study is more effective than the direct method without HV^{2+},[8] although the excitation of ZnTPP was common for both methods.

(18) (a) Walsh, J. L.; Baumann, J. A.; Meyer, T. J. *Inorg. Chim. Acta* **1980**, *19*, 2145−2151. (b) Toma, H. E.; Cunha, C. J.; Cipriano, C. *Inorg. Chim. Acta* **1988**, *154*, 63−66.

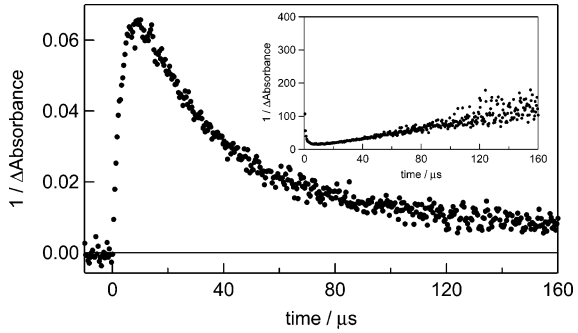

Figure 5. Decay-time profile of $[Ru_3(\mu_3\text{-}O)(\mu\text{-}CH_3CO_2)_6(cpy)_3]^0$ at 940 nm. Inset: Second-order plot of back-electron transfer of $[Ru_3(\mu_3\text{-}O)(\mu\text{-}CH_3CO_2)_6(cpy)_3]^0$ with $ZnTPP^{\bullet+}$ in AN.

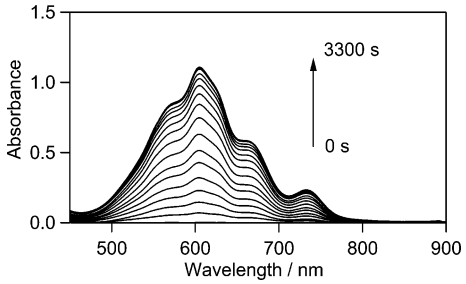

Figure 6. Steady-state absorption spectra changes under photoirradiation of ZnTPP (0.05 mM) in the presence of HV^{2+} (0.1 mM) and BNAH (0.1 mM) in Ar-saturated AN.

In the long time-scale measurements, $[Ru_3(\mu_3\text{-}O)(\mu\text{-}CH_3CO_2)_6L_3]^0$ began to decay slowly after reaching a maximum at ca. 10 μs as shown in Figure 5. The decay of $[Ru_3(\mu_3\text{-}O)(\mu\text{-}CH_3CO_2)_6L_3]^0$ obeys second-order kinetics, suggesting that the bimolecular back-electron transfer takes place with $ZnTPP^{\bullet+}$ as shown in eq 6.

$$ZnTPP^{\bullet+} + [Ru_3(\mu_3\text{-}O)(\mu\text{-}CH_3CO_2)_6L_3]^0 \xrightarrow{k_{BET}^{final}} ZnTPP + [Ru_3(\mu_3\text{-}O)(\mu\text{-}CH_3CO_2)_6(L)_3]^+ \quad (6)$$

From the slope of the second-order plots in the inset of Figure 5, the final back-electron transfer rate constants (k_{BET}^{final} in eq 6) were evaluated as listed in Table 1.

Upon the addition of BNAH as a sacrificial donor, the back-electron transfer process of eq 2 is expected to be retarded by consuming $ZnTPP^{\bullet+}$ with BNAH. Indeed, the accumulation of $HV^{\bullet+}$ was observed by the continuous irradiation of ZnTPP in the presence of HV^{2+} and BNAH as shown in Figure 6, although in the absence of BNAH, such accumulation of $HV^{\bullet+}$ was not observed.

When $[Ru_3(\mu_3\text{-}O)(\mu\text{-}CH_3CO_2)_6L_3]^+$ was added to this solution in the dark, the generation of $[Ru_3(\mu_3\text{-}O)(\mu\text{-}CH_3CO_2)_6L_3]^0$ was observed as shown in Figure 7. The concentration of $[Ru_3(\mu_3\text{-}O)(\mu\text{-}CH_3CO_2)_6L_3]^0$ increased with the concentration of $[Ru_3(\mu_3\text{-}O)(\mu\text{-}CH_3CO_2)_6L_3]^+$ under the conditions of $[HV^{\bullet+}] > [[Ru_3(\mu_3\text{-}O)(\mu\text{-}CH_3CO_2)_6L_3]^+]$. Then, we finally obtained persistent $[Ru_3(\mu_3\text{-}O)(\mu\text{-}CH_3CO_2)_6L_3]^0$ upon starting from the photoexcitation of ZnTPP in the presence of HV^{2+}, $[Ru_3(\mu_3\text{-}O)(\mu\text{-}CH_3CO_2)_6L_3]PF_6$, and BNAH.

To understand the photosensitized electron-transfer processes, the energy diagram can be illustrated as shown in Figure 8. The energy level of radical ions $ZnTPP^{\bullet+}$ and $HV^{\bullet+}$

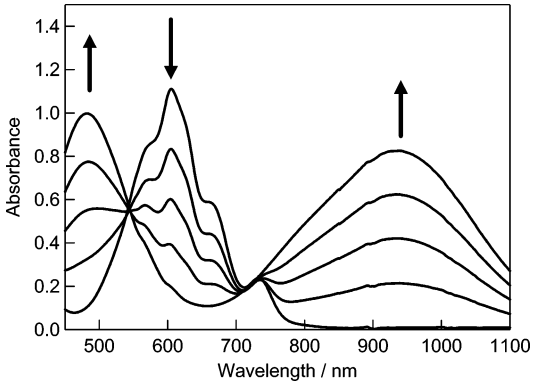

Figure 7. Steady-state absorption spectral changes when $[Ru_3(\mu_3\text{-}O)(\mu\text{-}CH_3CO_2)_6(cpy)_3]^+$ was added by steps (0, 0.01, 0.02, 0.04, and 0.05 mM) in the dark to the solution (3300 s) in Figure 6.

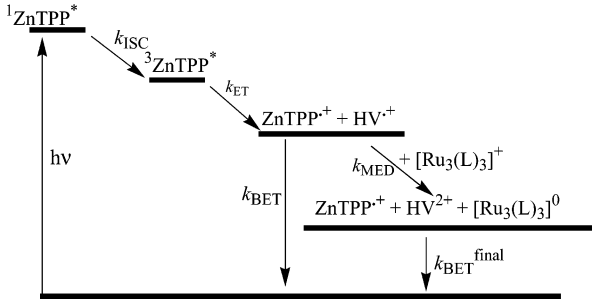

Figure 8. Energy diagram for photosensitizing electron-transfer and electron-mediating processes of ZnTPP, HV^{2+}, and $[Ru_3(L)_3]^+$.

Scheme 1. Photoinduced Processes of ZnTPP, $[Ru_3(\mu_3\text{-}O)(\mu\text{-}CH_3CO_2)_6(L)_3]^+$, and HV^{2+}

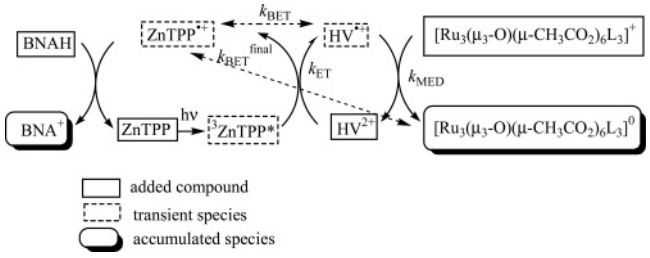

was evaluated by the Rehm−Weller equation[16] to be 1.23 eV, which is lower than the energy level of $^3ZnTPP^*$. The energy level of radical ions $ZnTPP^{\bullet+}$ and $[Ru_3(\mu_3\text{-}O)(\mu\text{-}CH_3CO_2)_6L_3]^0$ is even lower than that of radical ions $ZnTPP^{\bullet+}$ and $HV^{\bullet+}$, supporting the easy electron-mediating process. Finally, BNAH consumes $ZnTPP^{\bullet+}$, generating ZnTPP and BNA^+,[19] leaving $[Ru_3(\mu_3\text{-}O)(\mu\text{-}CH_3CO_2)_6L_3]^0$ as the sole species, which is potentially higher than the starting species, $[Ru_3(\mu_3\text{-}O)(\mu\text{-}CH_3CO_2)_6L_3]^+$. Therefore, $[Ru_3(\mu_3\text{-}O)(\mu\text{-}CH_3CO_2)_6L_3]^0$ can be act electron poor.

These processes are illustrated in Scheme 1, which clearly shows all the kinetic processes for the photosensitizing electron-transfer and electron-mediating cycle. Therefore, we established a novel system to accumulate $[Ru_3(\mu_3\text{-}O)(\mu\text{-}CH_3CO_2)_6L_3]^0$ by the photoexcitation of ZnTPP as photosensitizing electron donor in the presence of HV^{2+} as an electron-

(19) (a) Fukuzumi, S.; Inada, O.; Suenobu, T. *J. Am. Chem. Soc.* **2002**, *124*, 14538−14539. (b) Zhu, X.; Li, H.; Qian, L.; Ai, T.; Lu, J.; Yang, Y.; Cheng, J. *Chem.—Eur. J.* **2003**, *9*, 871−880. (c) Fukuzumi, S.; Inada, O.; Suenobu, T. *J. Am. Chem. Soc.* **2003**, *125*, 4808−4816.

mediating reagent and BNAH as sacrificial donor to reproduce ZnTPP from $ZnTPP^{\bullet+}$.

Conclusion

In the present study, we demonstrated an enhancement of photoinduced electron-accepting efficiency of tris-nuclear ruthenium complexes by the combination of the photosensitizing electron-transfer process with the electron-mediating process, which avoids unnecessary excited-energy deactivation processes without electron transfer. In the irreversible electron transfer, using BNAH as the sacrificial donor system, radical species such as $ZnTPP^{\bullet+}$ and $HV^{\bullet+}$ return to the original state, leaving the reduced form of $[Ru_3(\mu_3\text{-}O)(\mu\text{-}CH_3CO_2)_6L_3]^+$, persistently. These processes can be widely applied to the photoinduced electron-transfer processes using the tris-ruthenium complexes. For example, the application of the tris-ruthenium complex with high electron-accepting ability removing the electron from the electrode surface[20] may be possible under photoillumination.

Acknowledgment. This research was partially supported by Grant-in-Aid for the COE project, "Giant Molecules and Complex Systems", 2002. This work was also supported by a Grant-in-Aid for Scientific Research on Priory Area (417) from the Ministry of Education, Culture, Sports, Science, and Technology (NEXT) of Japan.

IC050960S

(20) (a) Abe, M.; Michi, T.; Sato, A.; Kondo, T.; Zhou, W.; Ye, S.; Uosaki, K.; Sasaki Y. *Angew. Chem., Int. Ed.* **2003**, *42*, 2912−2915. (b) Ye, S.; Zhou, W.; Abe, M.; Nishida, T.; Cui, L.; Uosaki, K.; Osawa, M.; Sasaki, Y. *J. Am. Chem. Soc.* **2004**, *126*, 7434−7435.